An application of A Multi-layer Zone Model to A Tunnel fire

Keichi Suzuki[1], Takeyoshi Tanaka[2], Kazunori Harada[3], and Harunori Yoshida[4]

[1]*Institute of Technology, Shimizu Construction Corporation 3-4-17 Echujima Koto-ku, Tokyo 135-8530, Japan*
[2]*Disaster Prevention Research Institute, Kyoto University Gokasho, Uji, Kyoto 611-0011, Japan*
[3]*Department of Architecture and Architectual Systems, Graduate School of Eng., Kyoto University Yoshidahonmachi, Sakyo-ku, Kyoto 606-8501, Japan*
[4]*Department of Urban and Environmental Eng., Graduate School of Eng., Kyoto University Yoshidahonmachi, Sakyo-ku, Kyoto 606-8501, Japan*

Abstract

In this study, a new zone modeling approach, which we call a MLZ model, is addressed to predict vertical distributions of temperature and chemical species concentrations in a tunnel fire. In this model the space volume in a tunnel is divided into an arbitrary number of areas and layers as the control volumes, and the physical properties, such as temperature and species concentrations, in each layer of each area are assumed to be uniform. The boundary walls are also divided into segments in accordance with the layer division and the radiation heat transfer between the layers and between the layers and the wall segments are calculated, as well as the convective heat transfer between the layers and the wall segments. This model still retains the advantage of zone models in terms of computational loaded so is expected to be useful for practical applications associated with fire safety design of tunnels. The calibration and verification of the model against an experiment with small tunnel facility are presented, then predicted temperatures generally show satisfactory agreement with the experiments.

1. INTRODUCTION

Recently, computational fluid dynamics (CFD) models are applied to some major tunnels for designing fire protection and smoke control system [1]. They can calculate the temperature and velocity field and predict the smoke movement in the fire, throughout the domain of interest. Three-dimensional time-dependent equations describing the laws of fluid dynamics are solved numerically with the surface conditions specific to the problem. An advantage of the models is that they can predict detailed distributions of temperatures and velocities in the domain of interest. On the other hand, CFD models need tremendous CPU

time. In a complicated case, it can be more than a couple of days for only 1 minute of simulation time.

The other methods available for predicting the smoke movement are zone models, which are used frequently for building fire issue. It assumes that a compartment consists of one layer or two, and that the physical properties of each layer, such as gas temperature and species concentrations are uniform. In the case of the two-layer zone models, the interface of the layers changes in height according to the mass inputs through a fire plume and heat transfer[2]. In a tunnel fire experiment, while a stratified layer situation can be observed, the layer interface is not always clear and the temperature varies rather gradually with height and distance from the fire origin. So if there is model which can predict the vertical temperature profile, more accurate analyses of smoke movement can be made possible within a practical computation time.

In this study, a new zone modeling approach, which we call a multi-layer zone model (MLZ model)[3], was applied to predict vertical distributions of temperature and chemical species concentrations in a tunnel fire. In this model the space volume in a tunnel is divided into an arbitrary number of regions consisting multiple horizontal layers as the control volumes, as illustrated in Fig.1, and the physical properties, such as the temperature and the species concentrations, in each layer of each region are assumed to be uniform. The boundary walls are also divided into segments in accordance with the layer division and the radiation heat transfer between the layers and between the layers and the wall segments are calculated, as well as the convective heat transfer between the layers and the wall segments. This model still retains the advantage of zone models in terms of computational load so is expected to be useful for practical applications associated with fire safety design of tunnels.

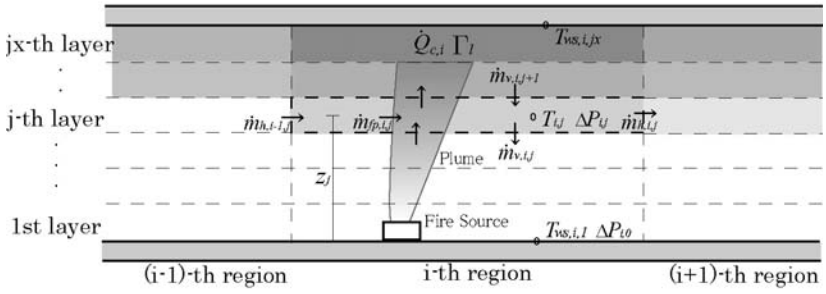

Fig.1 The concept of MLZ model to a tuunel fire

2. THE MODEL

The concept of the MLZ model for tunnel problems is demonstrated in Fig.1. One of the notable differences of the concept of the model from the existing two-layer zone models is

that the fire plume flow does not mix with the upper layer at a layer interface but continues to rise until it hits the ceiling, after which it pushes down the gases in the top layer and flow horizontally.

2.1 Zone Conservations

The principal equations of ordinary two-layer zone models were derived from the conservation equations of mass and energy for the upper and lower layers in the each region. In the case of the multi-layer zone model, the conservation equations for each laminated horizontal layer are also the bases to derive the equations. These conservation equations for mass, internal energy, and species fraction, are as follows:

(1) Mass conservation

$$\frac{d}{dt}\left(\rho_{i,j}V_{i,j}\right) = -\dot{m}_{fp,i,j} + \dot{m}_{h,i-1,j} - \dot{m}_{h,i,j} + \dot{m}_{v,i,j+1} - \dot{m}_{v,i,j} \tag{1}$$

where $\rho_{i,j}$ [kg/m^3] and $V_{i,j}$ [m^3] are the density and the volume of the j-th $(1 \le j \le jx-1)$ layer of i-th region, $\dot{m}_{fp,i,j}$ [kg/s] is the mass flow rate entrained into the fire plume from it. $\dot{m}_{v,i,j}$ [kg/s] is the mass flow rate from the j-th layer to the (j-1)-th through the surface outside of the fire plume, $\dot{m}_{h,i,j}$ [kg/s] is the horizontal mass flow rate flowing out through the boundary from the i-th layer to the (i+1)-th layer. For the top layer, considering that the mass rate of gas entrained into the fire plume is eventually transported to the layer, the mass conservation becomes as follows:

$$\frac{d}{dt}\left(\rho_{i,jx}V_{i,jx}\right) = \sum_{j=1}^{jx-1}\dot{m}_{fp,i,j} - \dot{m}_{v,i,jx} + \dot{m}_{h,i-1,jx} - \dot{m}_{h,i,jx} \tag{2}$$

where subscript *jx* stands for the top layer.

(2) Energy conservation

$$\frac{d}{dt}\left(C_p\rho_{i,j}V_{i,j}T_{i,j}\right) = -C_p\dot{m}_{fp,i,j}T_{i,j} + h_{v,i,j+1} - h_{v,i,j} + h_{h,i-1,j} - h_{h,i,j} - \dot{Q}_{w,i,j} - \dot{Q}_{r,i,j} \tag{3}$$

where C_p [kJ/kgK] is the specific heat, $T_{i,j}$ [K] is the temperature of the j-th layer of the i-th region, $\dot{Q}_{w,i,j}$ [kW] is the convection heat loss to the wall surface and $\dot{Q}_{r,i,j}$ [kW] is the net radiation heat loss from the j-th layer of the i-th region. If $\dot{m}_{v,i,j}$ is positive, the net flow through the interface of the (j+1)-th and the i-th layers is downward, otherwise upward. Then $h_{v,i,j}$ [kW] deals with the change of the direction of the flow with the manner as follows:

$$h_{v,i,j} = \begin{cases} C_p\dot{m}_{v,i,j}T_{i,j} & \left(\dot{m}_{v,i,j} > 0\right) \\ C_p\dot{m}_{v,i,j}T_{i,j-1} & \left(\dot{m}_{v,i,j} \le 0\right) \end{cases} \tag{4}$$

If $\dot{m}_{h,i,j}$ is positive, the net flow through the interface of the i-th and the (i+1)-th regions is rightward, otherwise leftward. Then $h_{h,i,j+1}$ [kW] deals with the change of the direction of the flow with the manner as follows:

$$h_{h,i,j}=\begin{cases} C_p\dot{m}_{h,i,j}T_{i,j} & \left(\dot{m}_{h,i,j}>0\right) \\ C_p\dot{m}_{h,i,j}T_{i+1,j} & \left(\dot{m}_{h,i,j}<0\right) \end{cases} \tag{5}$$

For the top layer, considering that the heat released by the combustion is transported to the layer through the fire plume, $\dot{Q}_{c,i}$ [kW], the energy conservation of the i-th region, is written as

$$\frac{d}{dt}\left(C_p\rho_{i,jx}V_{i,jx}T_{i,jx}\right)=\sum_{j=1}^{jx-1}C_p\dot{m}_{fp,i,j}T_{i,jx}+\dot{Q}_{c,i}-h_{v,i,jx}+h_{h,i-1,jx}+h_{h,i,jx}-\dot{Q}_{w,i,jx}-\dot{Q}_{r,i,jx} \tag{6}$$

(3) Species conservation

$$\frac{d}{dt}\left(\rho_{i,j}V_{i,j}Y_{l,i,j}\right)=-\dot{m}_{fp,i,j}Y_{l,i,j}+M_{l,v,i,j+1}-M_{l,v,i,j}+M_{l,h,i-1,j}-M_{l,h,i,j} \tag{7}$$

where $Y_{l,i,j}$ [kg/kg] is the mass fraction of the species *l* in the j-th layer of the i-th region, $M_{l,v,i,j}$ [kg/s] and $M_{l,h,i,j}$ [kg/s] deal with the change of the direction of the flow with the manner as follows:

$$M_{l,v,i,j}=\begin{cases} \dot{m}_{v,i,j}Y_{l,i,j} & \left(\dot{m}_{v,i,j}>0\right) \\ \dot{m}_{v,i,j}Y_{l,i,j-1} & \left(\dot{m}_{v,i,j}<0\right) \end{cases} \quad \text{and} \quad M_{l,h,i,j}=\begin{cases} \dot{m}_{h,i,j}Y_{l,i,j} & \left(\dot{m}_{h,i,j}>0\right) \\ \dot{m}_{h,i,j}Y_{l,i+1,j} & \left(\dot{m}_{h,i,j}<0\right) \end{cases} \tag{8}$$

For the top layer, considering that all the fire effluent generated by the fore source are all transported to the layer by the fire plume, the species conservation is given by

$$\frac{d}{dt}\left(\rho_{i,jx}V_{i,jx}Y_{l,i,jx}\right)=\sum_{j=1}^{jx-1}\dot{m}_{fp,i,j}Y_{l,i,j}+\Gamma_{l,i}-M_{l,i,jx}+M_{l,i-1,jx}-M_{l,i,jx} \tag{9}$$

where $\Gamma_{l,i}$ is the mass production rate of the species *l* by the fire source.

(4) Equation of state

Considering that a fire is basically a phenomenon at atmospheric pressure, the equation of state of the ideal gas in this model is simplified as follows:

$$\rho_{i,j}T_{i,j}=const. \tag{10}$$

2.2 Governing Equations for Zone Properties

Noting that the left-hand side of Eq.3 can be expanded as follows:

$$\frac{d}{dt}\left(C_p\rho_{i,j}V_{i,j}T_{i,j}\right)=C_p\rho_{i,j}V_{i,j}\frac{dT_{i,j}}{dt}+C_pT_{i,j}\frac{d}{dt}\left(\rho_{i,j}V_{i,j}\right) \tag{11}$$

the zone governing equation for temperature of each layer is derived by substituting Eqs.1 and 3 into Eq.11 and arranging, as follows:

$$\frac{dT_{i,j}}{dt}=\frac{1}{C_p\rho_{i,j}V_{i,j}}\Big(h_{v,i,j+1}-C_p\dot{m}_{v,i,j+1}T_{i,j}-h_{v,i,j}+C_p\dot{m}_{v,i,j}T_{i,j} \\ +h_{h,i-1,j}-C_p\dot{m}_{h,i-1,j}T_{i,j}-h_{h,i,j}+C_p\dot{m}_{h,i,j}T_{i,j}-\dot{Q}_{w,i,j}-\dot{Q}_{r,i,j}\Big) \tag{12}$$

For the top layer, substituting Eqs.2 and 6 into Eq.11 yields

$$\frac{dT_{i,jx}}{dt}=\frac{1}{C_p\rho_{i,jx}V_{i,jx}}\Bigg(\sum_{j=1}^{jx-1}\dot{m}_{fp,i,j}T_{i,j}-T_{i,jx}\sum_{j=1}^{jx-1}\dot{m}_{fp,i,j}+\dot{Q}_{c,i}-h_{v,i,jx}+C_p\dot{m}_{v,i,jx}T_{i,jx} \\ +h_{h,i-1,jx}-C_p\dot{m}_{h,i-1,jx}T_{i,jx}-h_{h,i,jx}+C_p\dot{m}_{h,i,jx}T_{i,jx}-\dot{Q}_{w,i,jx}-\dot{Q}_{r,i,jx}\Big) \tag{13}$$

Likewise, the zone governing equation for mass fraction of species *l* in each layer is derived by arranging Eq.1 and 7 as follows:

$$\frac{dY_{l,i,j}}{dt}=\frac{1}{\rho_{i,j}V_{i,j}}\Big(M_{l,v,i,j+1}-\dot{m}_{v,i,j+1}Y_{l,i,j}-M_{l,v,i,j}+\dot{m}_{v,i,j}Y_{l,i,j} \\ +M_{l,h,i-1,j}-\dot{m}_{h,i-1,j}Y_{l,i,j}-M_{l,h,i,j}+\dot{m}_{h,i,j}Y_{l,i,j}\Big) \tag{14}$$

For the top layer, arranging Eq.1 and 8 yields

$$\frac{dY_{l,i,jx}}{dt}=\frac{1}{\rho_{i,jx}V_{i,jx}}\Bigg(\sum_{j=1}^{jx-1}\dot{m}_{fp,i,j}Y_{l,i,j}-Y_{l,i,jx}\sum_{j=1}^{jx-1}\dot{m}_{fp,i,j}-M_{l,v,i,jx}+\dot{m}_{v,i,jx}Y_{l,i,jx} \\ +M_{l,h,i-1,jx}-\dot{m}_{h,i-1,jx}Y_{l,i,jx}-M_{l,h,i,jx}+\dot{m}_{h,i,jx}Y_{l,i,jx}\Big) \tag{14'}$$

2.3. Mass Transport

To Solve the equations for the temperature and species mass fraction of each layer, Eqs.10, 11, 13 and 14, the rate terms in them must be formulated based on the relevant modeling of component processes of fire. This section deals with the modeling of the mass flow rates involved.

(1) Mass flow rate through opening

Adding the energy conservation equations, Eq.1, of all layers, and Eq.2, of the top layer, we have the mass conservation equations of each region at each time step, as follows:

$$\sum_{j=1}^{jx}\Big(h_{h,i-1,j}-h_{h,i,j}-\dot{Q}_{w,i,j}-\dot{Q}_{r,i,j}\Big)+\dot{Q}_{c,i}=0 \tag{15}$$

The pressure differences between the compartment and outside at the mean height of the j-th layer from the floor of the i-th region, $\Delta P_{i,j}$ [Pa], is computed as

$$\Delta P_{i,j}=\Delta P_{i,0}-g\sum_{k=1}^{j}\rho_{i,k}\Delta z+g\rho_0 z_j \tag{16}$$

where $\Delta P_{i,0}$ is the pressure difference at the floor level of the i-th region, g is the acceleration due to gravity, Δz [m] is the thickness of layers ρ_0 is the density of the

standard air and z_j [m] is the mean height of the i-th layer from the floor. Then $\dot{m}_{h,i,j}$ is computed layer by layer, using $\Delta P_{i,j}$ [Pa] as

$$\dot{m}_{h,i,j} = \begin{cases} \alpha_v A_{b,i,j} \sqrt{2\rho_{i,j}\left(\Delta P_{i,j} - \Delta P_{i+1,j}\right)} & \left(\Delta P_{i,j} - \Delta P_{i+1,j} \geq 0\right) \\ \alpha_v A_{b,i,j} \sqrt{2\rho_{i+1,j}\left(\Delta P_{i+1,j} - \Delta P_{i,j}\right)} & \left(\Delta P_{i,j} - \Delta P_{i+1,j} < 0\right) \end{cases} \quad (17)$$

where α_v is the flow coefficient, $A_{b,i,j}$ [m^2] is the area of the boundary of the j-th layer between i-th and (i+1)-th region.

Eq.15 includes the pressures at the floor level of the i-th and (i-1)-th regions, $\Delta P_{i,0}$ and $\Delta P_{i-1,0}$, implicitly, because $h_{h,i,j}$ and $\dot{m}_{h,i,j}$ are determined as a function of them. The equation can be solved for the value of $\Delta P_{i,0}$ using an appropriate iteration method, such as Newton-Raphson method, i.e.: starting from an initial value of $\Delta P_{i,0}$ and calculating $h_{h,i,j}$ and $\dot{m}_{h,i,j}$ by Eq.17 and then substituting them into Eq.15, then modifying $\Delta P_{i,0}$ iteratively until the value of Eq.15 becomes close enough to zero. In this way, the pressure differences at the floor level of all regions, $\Delta P_{i,0}$, are calculated implicitly by Gauss-Seidel method, then, all horizontal flows are determined.

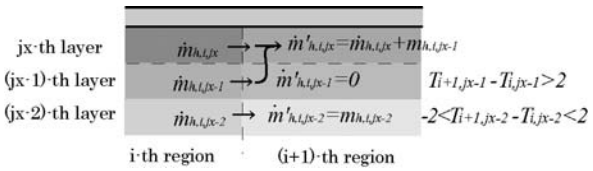

Fig.2 The weak plume through boundaries

A bi-directional flow at the boundary between regions will induce a weak plume because the gas temperature of the flow toward fire point is usually higher, shown as Fig.2. In this model, the entrainment of the gas into the weak plume is not considered at this moment. Instead, the mass flow through the boundary is simply assumed to be transported to the higher layer if the gas temperature of the flow is higher than the gas temperature of the layer than 2 Kelvin. If it is lower than 2 Kelvin, it was assumed to be transported to the lower layer. Then, the mass flow rate $\dot{m}_{h,i,j}$ transported by $\dot{m}'_{h,i,j}$, is calculated successively from one layer to another by the following equations.

$$\begin{cases} \dot{m}'_{h,i,j} = 0, \quad \dot{m}'_{h,i,j+1} = \dot{m}_{h,i,j+1} + \dot{m}_{h,i,j} & \left(T_{i,j} - T_{i+1,j} \geq 2\right) \\ \dot{m}'_{h,i,j} = \dot{m}_{h,i,j} & \left(-2 \leq T_{i,j} - T_{i+1} < 2\right) \\ \dot{m}'_{h,i,j} = 0, \quad \dot{m}'_{h,i,j-1} = \dot{m}_{h,i,j-1} + \dot{m}_{h,i,j} & \left(T_{i,j} - T_{i+1,j} < -2\right) \end{cases} \quad (18)$$

(2) Mass flow rate through surfaces of layers

The gas entrainment into the fire plume is important in smoke movement predictions. In this model, the mass flow rate of the fire plume at a layer interface is assumed to be given simply by the following equation with the entrainment coefficient of fire plume C_e, regardless the temperature of the plume ambient [4]:

$$\dot{m}_{fp,i,j} = C_e \dot{Q}_{c,i}^{1/3} \left(z_j^{5/3} - z_{j-1}^{5/3} \right) \quad (19)$$

The mass flow rate through the surface of the top layer to the lower layer outside of the fire plume, $\dot{m}_{v,i,jx}$, is obtained using Eq.2 as

$$\dot{m}_{v,i,jx} = \sum_{j=1}^{jx-1} \dot{m}_{fp,i,j} + \dot{m}_{h,i-1,jx} - \dot{m}_{h,i,jx} - \frac{d}{dt}\left(\rho_{i,jx} V_{i,jx}\right) \tag{20}$$

The mass flow rate through the interface of the (i+1)-th and the i-th layer, $\dot{m}_{v,i,j}$, is calculated layer by layer, using the enthalpy flow rate through the upper surface as follows:

$$\dot{m}_{v,i,j} = -\dot{m}_{fp,i,j} + \dot{m}_{v,i,j+1} + \dot{m}_{h,i-1,j} - \dot{m}_{h,i,j} - \frac{d}{dt}\left(\rho_{i,j} V_{i,j}\right) \tag{21}$$

2.4 Heat Transfer

(1) Convection heat transfer

The rate of the convection heat transfer from the j-th layer of the i-th region to the wall boundary, $\dot{Q}_{w,i,j}$, is calculated as follows:

$$\dot{Q}_{w,i,j} = \alpha_c (T_{i,j} - T_{ws,i,j}) A_{w,i,j} \tag{23}$$

where $T_{ws,i,j}$ is the temperature of the wall boundary around the i-th layer, and α_c is heat transfer coefficient of the wall on the layer[kW/K/m^2], which is assumed to be as follows [4]:

$$\overline{T} = \frac{T_{i,j} + T_{ws,i,j}}{2}$$

$$\alpha_c = \begin{cases} 0.005 & \left(\overline{T} \le 300\right) \\ 0.001(0.02\overline{T} - 1) & \left(300 < \overline{T} \le 800\right) \\ 0.015 & \left(800 < \overline{T}\right) \end{cases}$$

(2) Radiation heat transfer

The radiation heat flux from each layer consists of three directional components, i.e. the upward, the downward and the horizontal one, as shown in Fig.3. While the upward and downward radiation fluxes are exchanged between layers, with the upward flux from the top layer and the downward flux from the bottom layer as the only exceptions, where the heat fluxes are transferred to the walls. For simplicity, the horizontal flux is considered to be transferred only to the contacted wall boundary, not to the layers next regions.

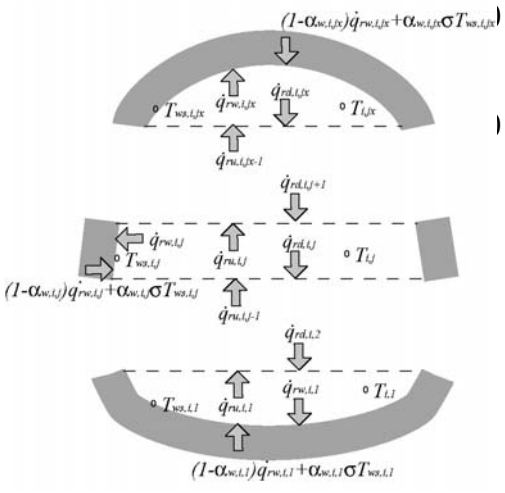

Fig.3 The image of radiation heat transfer

The procedure to solve the radiation heat loss $\dot{Q}_{r,i,j}$ is as follows; First, calculate the upward heat fluxes starting from the bottom layer, $\dot{q}_{ru,i,1}$[kW/m^2], then the flux starting from the i-th to the upper layer $\dot{q}_{ru,i,j}$ is calculated layer by layer from the bottom.

$$\dot{q}_{ru,i,1} = \alpha_{g,i,1}\sigma T_{i,1}^4 + \left(1-\alpha_{g,i,1}\right) F_{WU,i,1} \left\{(1-\alpha_{w,i,1})\dot{q}_{rw,i,1} + \alpha_{w,i,1}\sigma T_{ws,i,1}^4\right\} \tag{26}$$

$$\begin{aligned}\dot{q}_{ru,i,j} &= \left(1-\alpha_{g,i,j}\right) F_{LU,i,j}\dot{q}_{ru,i,j-1} + \alpha_{g,i,j}\sigma T_{i,j}^4 \\ &+ \left(1-\alpha_{g,i,j}\right) F_{WU,i,j} \left\{\left(1-\alpha_{w,i,j}\right)\dot{q}_{rw,i,j} + \alpha_{w,i,j}\sigma T_{ws,i,j}^4\right\} \qquad \left(j \neq 1, jx\right)\end{aligned} \tag{27}$$

where $\dot{q}_{rw,i,j}$ [kW/m^2] is the heat flux to the boundary of the wall, for which the value at the last time step is used, $F_{LU,i,j}$ and $F_{WU,i,j}$ are the view factors from the lower interface and the wall to the upper interface, $\alpha_{g,i,j}$ and $\alpha_{w,i,j}$ are the radiation absorptivity, which is the same as the emissivity, of the gas of the layer and of the wall surface contacting with it, respectively. Next, the downward heat flux from the top layer, $\dot{q}_{rd,i,jx}$ [kW/m^2] and from each layer, $\dot{q}_{rd,i,jx}$, are given layer by layer as follows:

$$\dot{q}_{rd,i,jx} = \alpha_{g,i,jx}\sigma T_{i,jx}^4 + \left(1-\alpha_{g,i,jx}\right) F_{WL,i,jx} \left\{(1-\alpha_{w,i,jx})\dot{q}_{rw,i,jx} + \alpha_{w,i,jx}\sigma T_{ws,i,jx}^4\right\} \tag{28}$$

$$\begin{aligned}\dot{q}_{rd,i,j} &= \left(1-\alpha_{g,i,j}\right) F_{UL,i,j}\dot{q}_{rd,i,j+1} + \alpha_{g,i,j}\sigma T_{i,j}^4 \\ &+ \left(1-\alpha_{g,i,j}\right) F_{WL,i,j} \left\{\left(1-\alpha_{w,i,j}\right)\dot{q}_{rw,i,j} + \alpha_{w,i,j}\sigma T_{ws,i,j}^4\right\} \qquad \left(j \neq 1, jx\right)\end{aligned} \tag{29}$$

where $F_{WL,i,j}$ and $F_{UL,i,j}$ are the view factors from the wall and upper surface to the lower surface, respectively. Next $\dot{q}_{rw,i,j}$ is obtained as follow:

$$\dot{q}_{rw,i,1} = \left(1-\alpha_{g,i,1}\right) F_{UW,i,1}\dot{q}_{rd,i,2} + \alpha_{g,i,1}\sigma T_{i,1}^4 \tag{30}$$

$$\dot{q}_{rw,i,j} = \left(1-\alpha_{g,i,j}\right)\left(F_{LW,i,j}\dot{q}_{ru,i,j-1} + F_{UW,i,j}\dot{q}_{rd,i,j+1}\right) + \alpha_{g,i,j}\sigma T_{i,j}^4 \quad \left(j \neq 1, jx\right) \tag{31}$$

$$\dot{q}_{rw,i,jx} = \left(1-\alpha_{g,i,jx}\right) F_{LW,i,jx}\dot{q}_{rd,i,jx-1} + \alpha_{g,i,jx}\sigma T_{i,jx}^4 \tag{32}$$

where the values calculated at the last step are used for $\dot{q}_{ru,i,j}$ and $\dot{q}_{rd,i,j}$, $F_{LW,i,j}$ and $F_{UW,i,j}$ are the view factors from the lower and the upper surface to the walls. Finally, the rate of radiation heat loss of the j-th layer of the i-th region is calculated layer by layer, using the values of the coefficients calculated at the current time step by

$$\begin{aligned}\dot{Q}_{r,i,j} &= -A_{f,i,j}\left(\dot{q}_{ru,i,j-1} - \dot{q}_{rd,i,j}\right) - A_{f,i,j+1}\left(-\dot{q}_{ru,i,j} + \dot{q}_{rd,i,j+1}\right) \\ &- A_{w,i,j}\left[\dot{q}_{rw,i,j} - \left\{\left(1-\alpha_{w,i,j}\right)\dot{q}_{rw,i,j} + \alpha_{w,i,j}\sigma T_{w,i,j}^4\right\}\right]\end{aligned} \tag{33}$$

Anyway, $\alpha_{g,i,j}$ changes according to the gas temperature and mass fractions of CO_2, H_2O and soot, of which the spectra are not uniform. In this model, the Fortran program ABSORB, developed by Modak [5], is used to calculate it.

(3) Conduction heat transfer

Conduction heat transfer in the wall is calculated, using a one-dimensional finite difference method. The governing equation is:

$$\frac{\partial T_{w,i,j}}{\partial t} = \frac{k_w}{c_w \rho_w} \frac{\partial^2 T_{w,i,j}}{\partial x^2} \tag{34}$$

where $T_{w,i,j}$ [K] is the temperature of the wall in contact with the j-th layer of i-th region, x [m] is the depth of the wall from the surface, t [s] is the time, k_w [kW/mK], c_w [kJ/kgK] and ρ_w [kg/m^3] are the thermal conductivity, the specific heat, and the density of the wall, respectively. The boundary conditions for the exposed and unexposed surface are as follows:

$$-k_w \left. \frac{\partial T_{w,i,j}}{\partial x} \right|_{x=0} = \frac{\dot{Q}_{w,i,j}}{A_{w,i,j}} + \dot{q}_{rw,i,j} \tag{35}$$

$$-k_w \left. \frac{\partial T_{w,i,j}}{\partial x} \right|_{x=l_w} = 0 \tag{36}$$

where l_w [m] is the depth to virtual adiabatic boundary. The depth must be predetermined for calculation, however in most cases of fire prediction it is not difficult to select the depth the larger than thermal penetration depth.

2.5 Combustion

(1) Heat release rate

Heat release rate due to the combustion of the fire source is given as,

$$\dot{Q}_{C,i} = C_b \dot{m}_{b,i} \Delta H \tag{37}$$

where $\dot{m}_{b,i}$ [kg/s] is the mass burning rate in the i-th region, ΔH [kW/kg] is the heat of combustion per unit fuel, and C_b is the coefficient of burning set to 0.65 in most cases, which means the efficiency of the heat transferred directly to the gas by the heat release rate assuming complete combustion.

(2) Chemical species generation

In this model, the generation and consumption of the chemical species Γ_l (l: soot, O_2, CO_2, H_2O, N_2) per unit fuel consumed in combustion are calculated by assuming a complete combustion.

2.6 Numerical Method

The structure of the computer program developed for numerically solving MLZ model is shown by the flow chart in Fig.3. For each time step, the zone equations, Eqs. 10, 11, 13 and 14, for the gas temperature and species fraction of each layer are solved by implicit method, combined with the subroutines for component physics.

3. COMPARISON WITH EXPERIMENTAL RESULTS

3.1 Experimental Data

In this section, the temperature data from 4 cases of the fire experiments in a small cylindrical tunnel equipment are compared with the predictions by the model. In the experiment, the vertical temperature distributions in some regions were measured by thermocouples. The horizontal wind speed from the one edge and the heat release rate were varied by cases. The parameter setting of each cases is shown in Tab.1. The diameter and length of the facility are 0.3m and 20 m, respectively, shown in Fig.4.

Tab.1 The Parameter set of the experiment and the calculation

	HRR[kW]	Vel.[m/s]	Ce
case1	0.5	0.16	0.12
case2	1.5	0.16	0.12
case3	0.5	0.48	0.19
case4	1.5	0.48	0.19

3.2 Conditions of Experiments

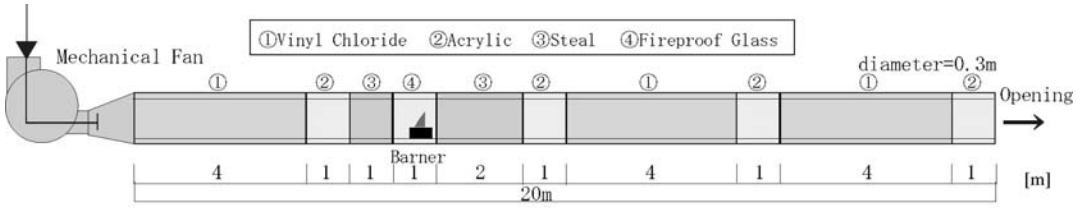

Fig.4 The experimental equipment

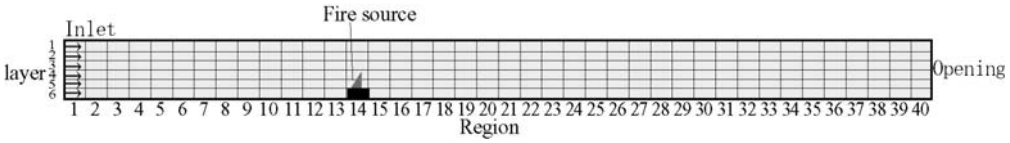

Fig.5 The domain of the calculation (longitudinal section)

The wall was vinyl chloride, acrylic, steal and fireproof glass, and the thickness were approximately 10 mm. Two levels of longitudinal air flow rate from the mechanical fan on the one edge, 0.16 m/s and 0.48 m/s, were applied in the experiments. Fig.4 shows the image of the experimental facility. The burner, which supplies propane at two fixed rates (equivalent to the heat release rates: 0.5kW, 1.5kW), was installed. The thermocouple trees, each of which has 7 measurement points (include one touched wall surface), were arrayed in the 14 points in the equipment. The temperatures were measured by thermocouples after 20 minutes from the ignition for steady state measurement.

3.3 Condition of the Calculation

The conditions of the calculations using the MLZ model, such as the geometry of the volume, the property of the walls, the initial air temperature in the domain and the heat release rate were

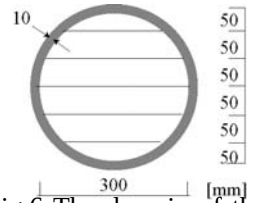

Fig.6 The domain of the calculation (side section)

determined basically according to the experimental conditions for each case, shown as Tab.1. The inlet boundary on the 1st region was set to a steady velocity of the parameter in each case and the temperature in the outside at the experiments. The volume in the domain divided into 40 regions and 6 layers, shown as Figs. 5 and 6. The physical calculation time step is 0.1 second. The plume entrainment coefficient C_e was set to 0.12 (case 1, 2) and 0.19 (case 3, 4), which is calculated by adding horizontal air flow effect to 0.08, the experimental value of windless field by Zukoski[4].

3.4 Analysis

Fig.8 shows the vertical distribution of the temperature from the experiment at steady state stage and predictions by the model at 1200 second (as almost steady-state) in case 1-4.

The predicted temperatures generally show satisfactory agreement with the experiments. However, (a) the temperatures in the upper part of the tunnel in Region 7 and 12 are lower, (b) the hot upper layers in Region 22 and 27are lower, and (c) the hot upper layers in the region 16 and 18 of case 9 and 19 are thicker by 0.05-0.10m than the experiments. One of the reasons of the former (a) is that the model can calculate only heat transfer due to net mass flow but couldn't calculate that due to diffusion and turbulence. The potential and probably the most plausible cause of (b) and (c) may

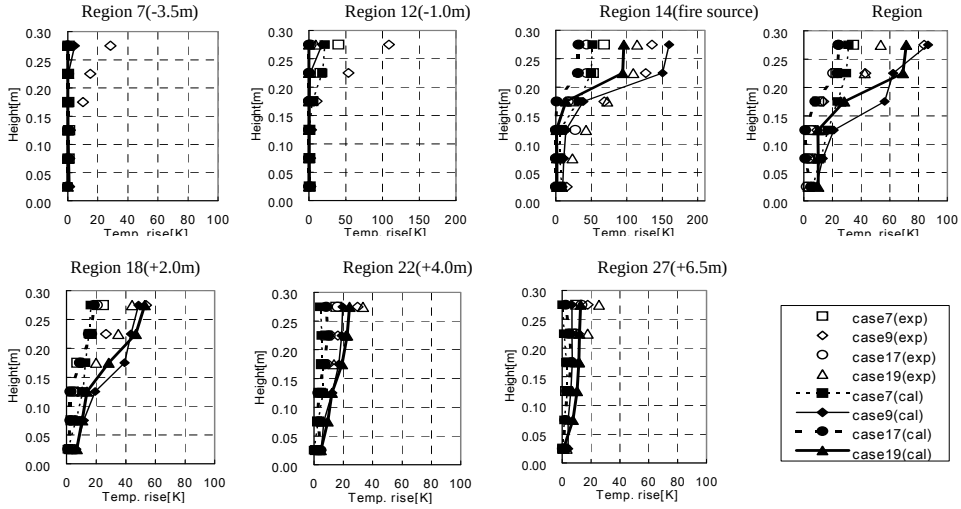

Fig. 7 The result of

be attributed to that the inertia force could not be considered for horizontal flow so it was calculated less and downward flow was calculated more. Then the hot layer were predicted thicker and the distribution of temperatures were flatter. Finally the CPU time of the calculation for each case is needed about 5 minutes by a PC with Pentium 4 1.9 GHz, of course, remarkably less than CFD.

4. CONCLUSION

In this study, the concept and mathematical formulation of a MLZ model were introduced. Unlike the existing two-layer zone models, this model allows to predict vertical distribution of temperature and species concentrations in a fire tunnel.

The results of the first stage comparison between the predictions and the experiments appear to be satisfactory and encouraging.

REFERENCES

[1] S. Kumar, “Field Model Simulation of Vehicle Fires in a channel Tunnel Shuttle Wagon ”, the 4-th Symposium of IAFSS, 1992.

[2] Tanaka, T. and Nakamura, K., “A Model for Predicting Smoke Transport in Buildings -Base on Two Layer Zone Concept –”, Building Research Institute, No.123, BRI, MOC, 1989.

[3] K. Suzuki, K. Harada and T. Tanaka, “A Multi-Layer Zone Model for Predicting Fire Behavior in a Single room”, the 6-th Symposium of IAFSS, Jun. 2001.

[4] Zukoski, E. E., “Smoke Movement and Mixing in Two-Layer Fire Models”, The 8th UJNR Joint Panel Meeting on Fire Research and Safety, Tsukuba, May. 1985.

[5] Modak, A. T.: “Radiation from products of Combustion”, Fire Research, 1, 1978/79